J Fluoresc (2016) 26:813–820
DOI 10.1007/s10895-016-1769-4

ORIGINAL ARTICLE

Green Emission of Tb-doped Mg-Al Layered Double Hydroxide Response to L-lysine

Yufeng Chen[1] · **Yao Bao**[1] · **Xiaoqing Wang**[1]

Received: 11 November 2015 / Accepted: 14 January 2016 / Published online: 20 January 2016

Abstract The paper describes a study on the green emission of a Tb-doped Mg-Al layered double hydroxide (Tb-LDH) response to L-lysine (Lys). Fluorescent study was found that the Tb-LDH exhibited strong green emission due to $^5D_4$-^7F_J (J = 5, 6) transition of Tb^{3+}, and the green emission almost quenched while the Tb-LDH was exposed to 0.01, 0.05, 0.1, 0.25, and 0.5 mol·L^{-1} Lys solution, respectively. Meanwhile the emission attributed to Lys markedly increased as the Tb-LDH was exposed to 0.01 and 0.05 mol·L^{-1} Lys solution, then decreased as the concentration of Lys solution further increased to 0.5 from 0.05 mol·L^{-1}. The green emission of Tb-LDH optimal response to Lys happened at 0.05 mol·L^{-1} of Lys solution. XRD results revealed that no reflections ascribed to Lys appeared in the composites of Tb-LDH and Lys. IR spectra suggested that the IR spectra of Tb-LDH obviously changed after it was exposed to Lys solution. These results indicated that the green emission of Tb-LDH response to Lys was possibly owing to interaction between the Tb-LDH and Lys. Moreover, this interaction between the Tb-LDH and Lys may be resulted from absorption. The green emission of Tb-LDH response to Lys would be potential application in detecting L-lysine.

Keywords Green emission · L-lysine · MgAl-LDH · Tb-doped · Response

✉ Yufeng Chen
yfchen@ncu.edu.cn

[1] College of Chemistry, Nanchang University, Nanchang 330031, China

Introduction

L-lysine (Lys) is an essential amino acid for animal and human nutrition. A Lys misbalanced diet entails severe diseases and so it is often added as a dietary supplement to foods and drugs. Lys content in foods or drugs can be used as an index of nutritional quality or for the evaluation of processing techniques [1]. Because Lys is easily damaged by thermal treatment and storage conditions, the development of the detection to Lys in food products or drugs is important. Despite some several methods have been described for lysine analysis or detection [2–5], these methods do not satisfy the requirements for an obvious and fast response. As it well known, rare earth ions have excellent luminescence [6, 7], long luminescence lifetime, and strong binding with biological molecules [8–10]. In view of the expensive rare earth elements compared with the common elements, Eu-doped Mg-Al LDH and Eu-doped Zn-Al LDH have been paid high attention [11, 12]. Moreover, the use of Eu-doped LDH as a fluorescent probe to detect amino acids with phenyl groups has been attempted [13, 14]. Although there are limited studies on Tb–complex intercalated into interlayer of MgAl-LDHs [15, 16], the investigation on Tb(III) doped onto layers of LDHs should be paid more attention because the Tb doped onto the layers of LDHs is more favorable for touching outer biological molecules compared with that of the Tb(III)–complex intercalated into interlayer of LDHs. For this reason, the Tb(III) was incorporated onto layers of MgAl-LDH and the green emission of Tb-doped Mg-Al LDH response to L-lysine was investigated in the present work. Meanwhile, the mechanism of the fluorescent response was probed.

Experimental

Materials Synthesis

$Tb(NO_3)_3$ solution (0.05 mol·L^{-1}) was prepared by Tb_2O_3 solid dissolved in mixed solution of concentrated HNO_3 and H_2O_2. The Tb-doped MgAl-LDH, with the molar ratios of Mg/(Al + Tb) of 2.0 and Tb/(Al + Tb) of 0.06, was synthesized by co-precipitation method [11, 12]. Namely the mixed solution of Mg^{2+}, Al^{3+}, and Tb^{3+} ions with certain molar ratio was prepared by $Mg(NO_3)_2{\cdot}6H_2O$ and $Al(NO_3)_3{\cdot}9H_2O$ solid dissolved in HNO_3 and mixed with $Tb(NO_3)_3$ solution. After the addition of 3.5 mol·L^{-1} NH_3 solution to the mixed solution, a precipitate formed (pH =8 ~ 9). Then the precipitant suspension was aged at 40 °C for two hours. After being filtrated, washed, and dried at 70 °C for 12 h, the Tb-doped MgAl-LDH was obtained (labeled as Tb-LDH).

Five Tb-doped MgAl-LDH aliquots ~1.0 g samples were added to 0.01, 0.05, 0.1, 0.25, and 0.5 mol·L^{-1} alkaline lysine aqueous solution, respectively, and kept on stirring at room temperature for 12 h. After the slurries were filtered, water-washed, and dried at 40 °C for 12 h, the corresponding products were labeled as Tb-LDH/Lys-1, Tb-LDH/Lys-2, Tb-LDH/Lys-3, Tb-LDH/Lys-4, and Tb-LDH/Lys-5. The physical mixture of Tb-doped LDH/Lys contained 0.5 g Tb-LDH and 0.5 g L-lysine solid powders. Ultra pure water was used in the whole experiment.

Characterization

X-ray diffraction (XRD) patterns were measured with X-ray diffractometer (XD-3, Beijing Puxi Tongyong Yiqi Ltd. China, CuK_α radiation). All the samples were scanned in the 2θ range of 3–70° at a scan rate of 2° /min. Chemical contents of Mg, Al, and Tb were determined by inductively coupled plasma atomic emission spectroscopy (ICP-AES Optima 5300DV American Pe Company, America) as well as scanning electron microscope equipped with energy dispersive X-ray analysis (SEM-EDX,

Table 1 Chemical compositions of Tb-LDH and Tb-LDH/Lys – n(n = 1, 2, 3, 4, 5)

Sample	[a]Molar ratio of $Mg^{2+}/(Al^{3+}+Tb^{3+})$	Basal spacing d_{003} (Å)	[b]Adsorbed Lys per 1 mol Tb-LDH
Tb-LDH	2.01	8.70	—
Tb-LDH/Lys-1	2.01	8.51	0.02
Tb-LDH/Lys-2	2.01	8.38	0.03
Tb-LDH/Lys-3	1.98	7.97	0.05
Tb-LDH/Lys-4	1.99	7.61	0.07
Tb-LDH/Lys-5	2.02	7.73	0.09

[a] ICP elemental analysis and EDX elemental analysis;

[b] CHN elemental analysis and calculated by charge balance principle

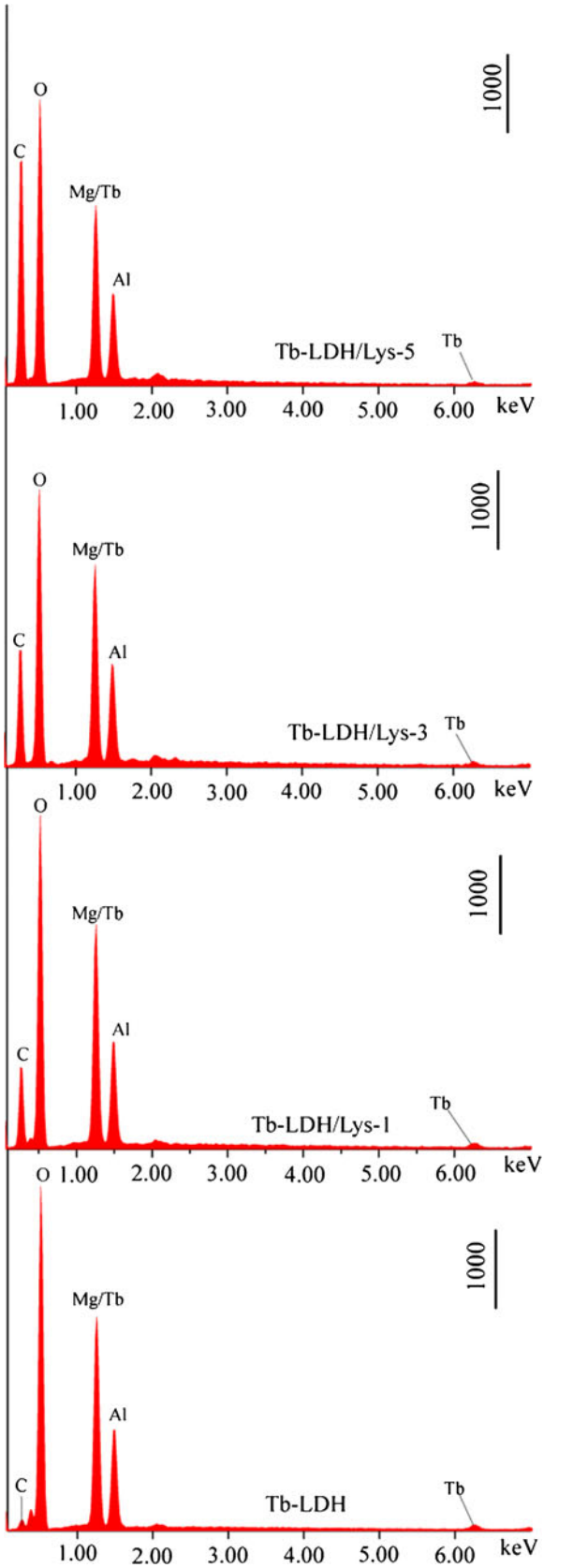

Fig. 1 EDX of Tb-LDH, Tb-LDH/Lys-1, Tb-LDH/Lys-3, and Tb-LDH/Lys-5

JEOL JSM-6701F). The C, H, and N contents of the Tb-LDH/Lys-n (n = 1, 2, 3, 4, 5) composites were determined by Element Analyzer (Elementar Vario EL II, Germany). Fourier transform infrared (FT-IR) spectra of the samples were surveyed by the KBr method using a FT-IR spectrometer (Himadzu IR Prestige-21). The fluorescent study was performed using a Spectrophotometer (F-7000 FL).

Result and Discussion

Compositional and Structural Analyses

The chemical compositions of Tb-LDH and Tb-LDH/Lys-n (n = 1, 2, 3, 4, 5) were determined by ICP, SEM-EDX, and CHN elemental analyses (seen in Table 1 and Fig. 1). According to elemental analyses and charge balance principle [17], the Tb-LDH/Lys-1, Tb-LDH/Lys-2, Tb-LDH/Lys-3, Tb-LDH/Lys-4, and Tb-LDH/Lys-5 contained 0.02, 0.03, 0.05, 0.07, and 0.09 mol lysine per 1 mol Tb-LDH, respectively, which is in accordance with the initial concentration of lysine solution. In addition, the molar ratio of $Mg^{2+}/(Al^{3+}+Tb^{3+})$ to be 2.0 was found in the Tb-LDH sample, which is in agreement with the initial ratio of raw reactants. Moreover, the $Mg^{2+}/(Al^{3+}+Tb^{3+})$ molar ratio of 2.0 kept in all the Tb-LDH/Lys-n (n = 1, 2, 3, 4, 5) composites, indicating the layers of Tb-LDH preservation during the reaction of Tb-LDH and lysine.

Figure 2 displays XRD patterns of Lys, Tb-LDH, mixture of Tb-LDH/Lys, and Tb-LDH/Lys-n (n = 1, 2, 3, 4, 5). The XRD pattern of Lys was in accordance with the literature [18], and the XRD pattern of Tb-LDH is similar to those of previous LDHs [17, 19–26]. The {003} basal plane space of 8.70 Å for the Tb-LDH is obviously larger than that of previous MgAl-LDHs [22–24]. This may due to the doped Tb, different $Mg^{2+}/(Al^{3+}+Tb^{3+})$ molar ratio, and interlayer anions, etc. After the Tb-LDH was exposed to 0.01, 0.05, 0.1, 0.25, and 0.5 mol·L^{-1} Lys solution, respectively, the basal spacing of the product Tb-LDH/Lys-n (n = 1, 2, 3, 4, 5) tended to decrease with the increase in the concentration of Lys solution. This result suggested the Lys not intercalated into interlayer spacing of Tb-LDH, but possibly adsorbed on surface of the Tb-LDH. However, the basal spacing is subject to various factors, including interlayer guest type, amount, and state, etc. It is very complicated to define the exact factor. The XRD pattern of the mixture of Tb-LDH/Lys appeared the reflections attributed to Tb-LDH and lysine. No reflections traceable to the Lys represented in the Tb-LDH/Lys-n(n = 1, 2, 3, 4, 5) composites. These results illustrated that the Lys is possibly amorphous or highly dispersed in the Tb-LDH/Lys-n composites. In addition, SEM images showed the morphology of Tb-LDH did not obviously change after the Tb-LDH reacted with different concentration of Lys solution (seen in Fig. 3), indicating the Tb-LDH not damaged by the alkaline L-lysine solution.

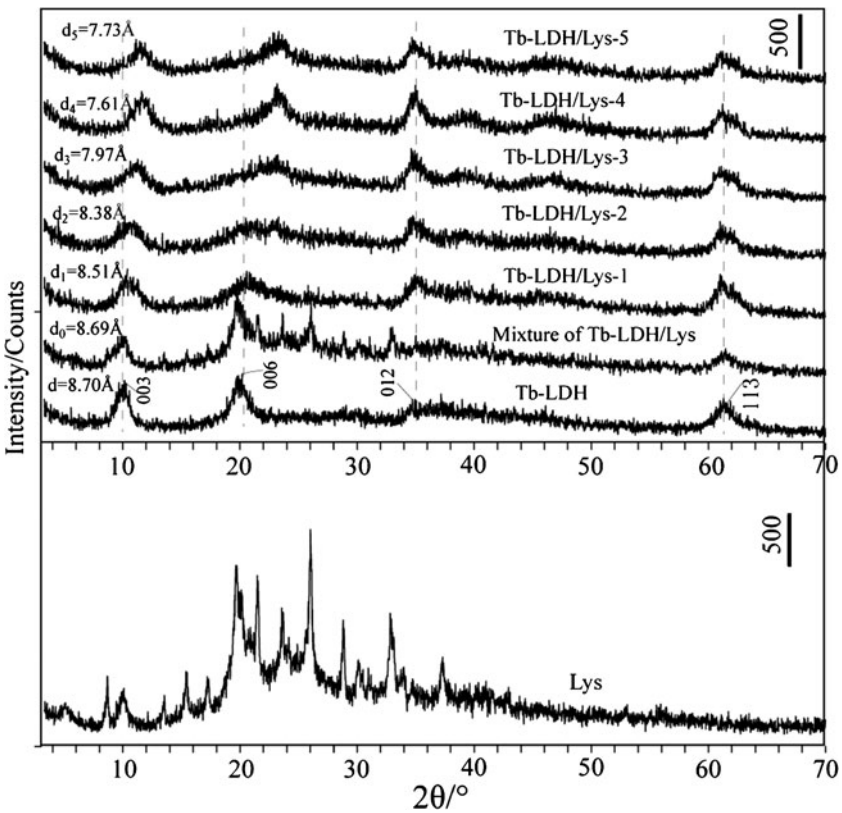

Fig. 2 XRD patterns of Lys, Tb-LDH, Mixture of Tb-LDH/Lys, Tb-LDH/Lys-1, Tb-LDH/Lys-2, Tb-LDH/Lys-3, Tb-LDH/Lys-4, and Tb-LDH/Lys-5

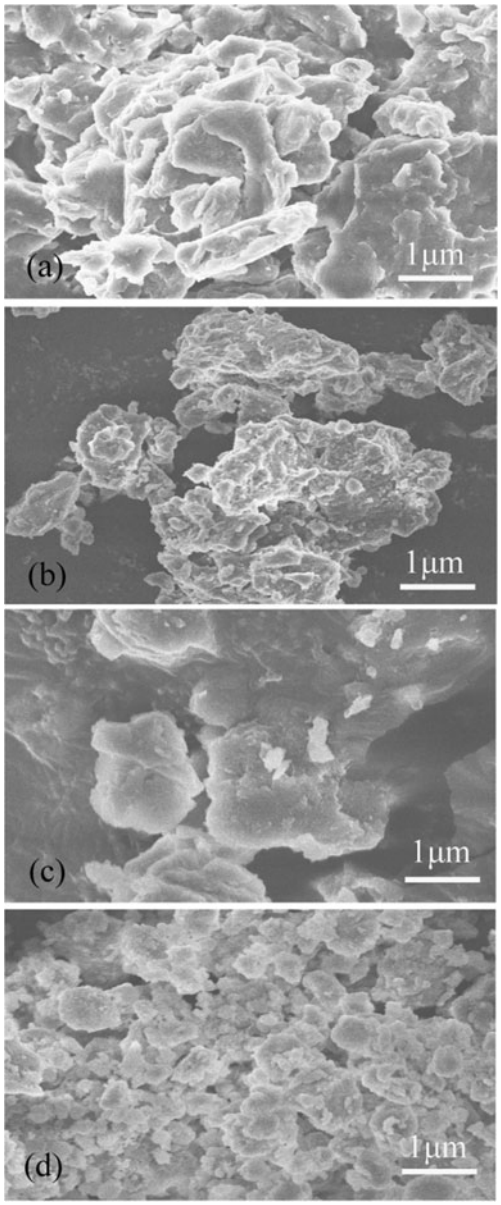

Fig. 3 SEM images of **a** Tb-LDH, **b** Tb-LDH/Lys-1, **c** Tb-LDH/Lys-3, and **d** Tb-LDH/Lys-5

IR Spectral Analysis

FT-IR spectra of Tb-LDH, Lys, mixture of Tb-LDH/Lys, and Tb-LDH/Lys-*n* (*n* = 1, 2, 3, 4, 5) present in Fig. 4. For the lysine (Lys) solid powder, the weak band around at 3402 is due to O–H group stretching vibration of water molecules [27]. Stretching vibrations of N-H bonds in the IR spectra are revealed as bands at 3046 and 2939 cm^{-1}, which is overlapped with strong band in the region of stretching vibrations of C-H bonds [27, 28]. In the region of asymmetric stretching vibration of carboxylate group and asymmetric deformation vibration of NH_3^+ groups there are peaks at 1635 and 1586 cm^{-1}. The band at 1504 cm^{-1} may be owing to symmetric deformation vibration of NH_3^+ groups, while the band at

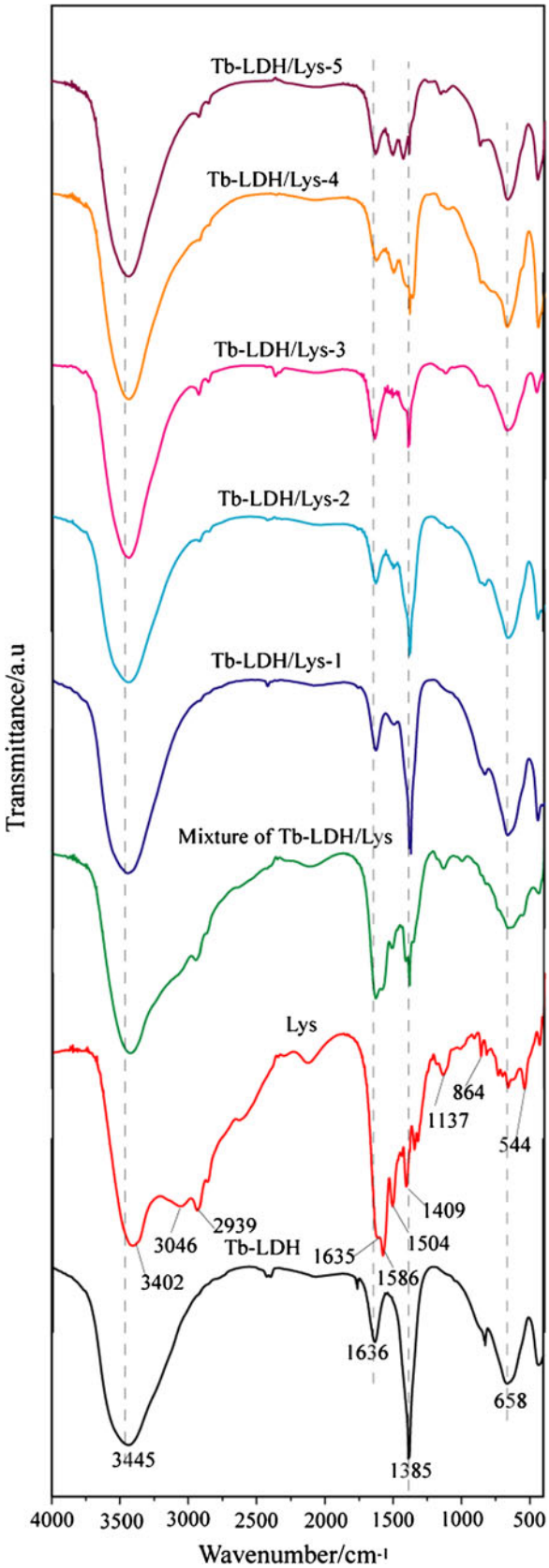

Fig. 4 IR spectra of Tb-LDH, Lys, Mixture of Tb-LDH/Lys, Tb-LDH/Lys-1, Tb-LDH/Lys-2,Tb-LDH/Lys-3, Tb-LDH/Lys-4, and Tb-LDH/Lys-5

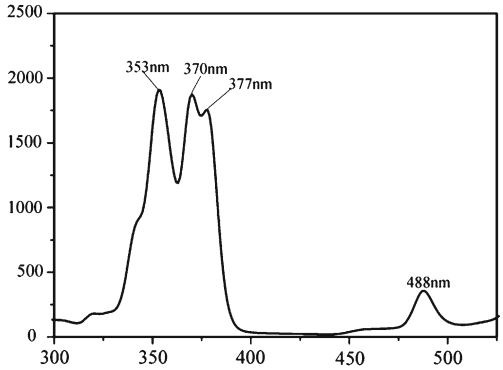

Fig. 5 Excitation spectrum of Tb-LDH (λ_{em} = 546 nm)

1409 cm^{-1} is ascribed to symmetric stretching vibration of carboxylate group [27–30]. The stretching vibration of the C-C group is observed at 1137 cm^{-1}, and C-C-N symmetric stretching appeared at 864 cm^{-1} [31]. With regard to Tb-LDH, the bands around at 3445 and 1636 cm-1 were assigned to O–H group stretching and bending vibrations of the hydroxide basal layer or interlayer water molecules [32]. The band at 1385 cm^{-1} may be due to deformation mode of carbonate ions absorbed [33]. The lattice vibration mode of the LDH sheets was observed at 658 cm^{-1} [34]. As expected, the IR spectrum of the mixture of Tb-LDH/Lys contained some bands attributed to Tb-LDH and Lys. In contrast to the mixture of Tb-LDH and Lys, the IR spectra of Tb-LDH/Lys-*n* were very different. Moreover, with the initial concentration of lysine solution varying from 0.01, 0.05, 0.1, 0.25, to 0.5 $mol \cdot L^{-1}$, the IR spectra of the Tb-LDH/Lys-*n* (n = 1, 2, 3, 4, 5) gradually changed. Two group of IR spectra can be found for the Tb-LDH/Lys-*n*(n = 1,2,3,4,5). One group consisted of Tb-LDH/Lys-1 and Tb-LDH/Lys-2, and their spectra are similar to that of the Tb-LDH; the other group contained Tb-LDH/Lys-3, Tb-LDH/Lys-4, and Tb-LDH/Lys-5, and their IR spectra are very different from that of the Tb-LDH. The bands attributed to lysine obviously present in the Tb-LDH/Lys-4 and Tb-LDH/Lys-5, which may be due to more lysine adsorbed by the Tb-LDH with the increase in the concentration of lysine solution.

Green Emission of Tb-LDH Response to lysine

The excitation spectrum was monitored for the 546 nm emissions of the Tb-LDH (Fig. 5), and four bands at 353, 370, 377, and 488 nm occurred, which is similar to the literature [35].

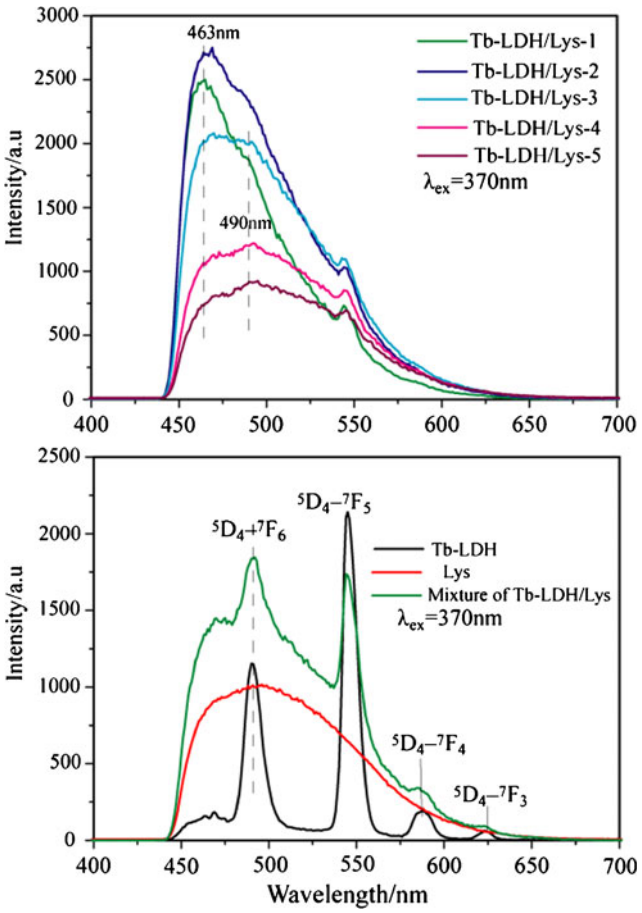

Fig. 6 Emission spectra of Tb-LDH, Lys, mixture of Tb-LDH/Lys, and Tb-LDH/Lys-n (n = 1, 2, 3, 4, 5) (λ_{ex} = 370 nm)

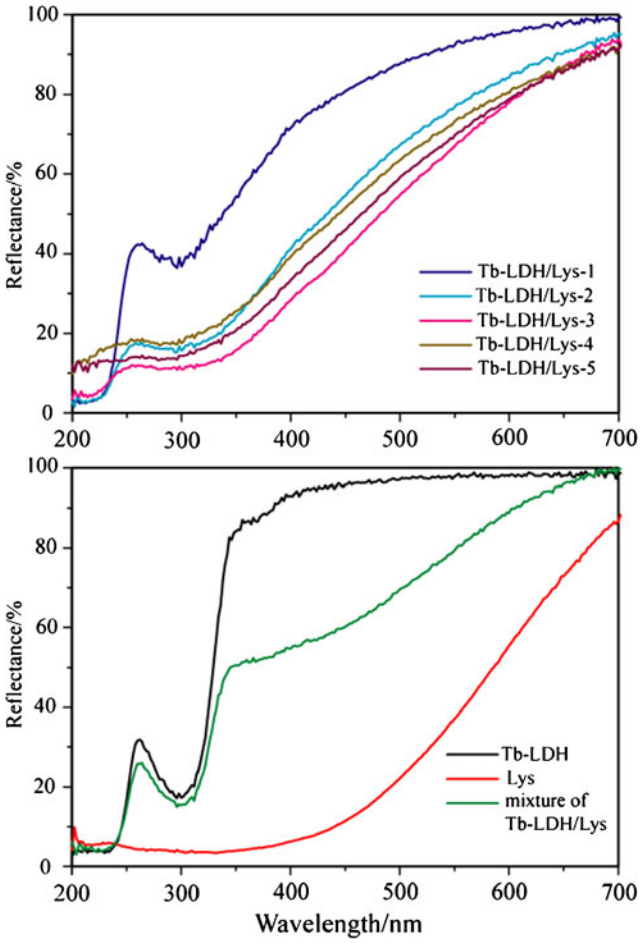

Fig. 7 UV-vis reflectance spectra of Tb-LDH, Lys, mixture of Tb-LDH/Lys, and Tb-LDH/Lys-n (n = 1, 2, 3, 4, 5

The bands at 353, 370, and 377 nm were attributed to $^7F_6 \rightarrow {}^5G_4$, $^7F_6 \rightarrow {}^5L_{10}$, and $^7F_6 \rightarrow {}^5G_6$ transitions, respectively [36, 37], while the band at 488 nm may be due to $^5D_4 \leftarrow {}^7F_6$ transition [38, 39]. Under the excitation of 370 nm wavelength, the Tb-LDH, Lys solid powders, mixture of Tb-LDH/Lys, and Tb-LDH/Lys-*n* (*n* = 1, 2, 3, 4, 5) were subject to measurement for the emission spectra. As shown in Fig. 6, the emissions attributed to $^5D_4$–^7F_J (J = 3, 4, 5, 6) transitions of Tb^{3+} were found in the Tb-LDH [40–42]. The most intense green emission attributed to $^5D_4$-$^7F_5$ transition of Tb^{3+} stands at 546 nm which is as strong as that of organic Tb-complexes [43–47]. The emission due to $^5D_4$-$^7F_5$ transition is hypersensitive to surroundings of Tb^{3+}, and the $^5D_4$-$^7F_6$ transition however has a magnetic dipole character and its intensity is almost independent of the environment of Tb^{3+}. For the Lys, a broad peak appeared at about 490 nm, which is similar to the literatures [48, 49]. As expected, the emissions attributed to Tb-LDH and Lys were observed in the mixture of Tb-LDH/Lys. As for the Tb-LDH/Lys-*n* (*n* = 1, 2, 3, 4, 5) composites, the emission owing to $^5D_4$-$^7F_5$ transition of Tb^{3+} markedly decreased and almost quenched, which indicated the green emission of Tb-LDH was sensitive to Lys (lysine). However, the emission attributed to Lys took on different changes when the Tb-LDH was exposed to different concentration of lysine solution. As the Tb-LDH was exposed to 0.01 and 0.05 mol·L^{-1} lysine solution, respectively, the emission attributed to $^5D_4$-$^7F_5$ transition of Tb^{3+} almost quenched, while the emission ascribed to Lys greatly increased, and obviously shifted to high energy (from 490 to 463 nm). With the increase in the concentration of lysine solution from 0.05, 0.1, 0.25, to 0.5 mol·L^{-1}, the increment in the emission ascribed to Lys gradually decreased, and the emission belonged to $^5D_4$-$^7F_5$ transition of Tb^{3+} still quenched. The result is against to most reports related to intramolecular energy transfer from ligand to metal ions, which can increase the luminescence of Tb^{3+} ions [50–54]. Some researchers think that fluorescence of Tb^{3+} (III) quenched by organic ligand is due to energy loss via the intersystem crossing channel from T_1 to singlet S_0 [39] or intramolecular back energy transfer from the $^5D_4$ (Tb^{3+}) state to the lowest triplets of the ligands [55]. In order to understand the fluorescent quenching, UV-visible reflectance spectra of samples represented in Fig. 7. The band-edge of the Tb-LDH exhibited in 320 ~ 375 nm in the light of the reflectance spectrum, which is in agreement with the result of excitation spectrum. The band-edge of the Lys was hardly defined from its reflectance spectrum due to poor crystallinity. As expected, the reflectance spectrum of the mixture of Tb-LDH/Lys combined the features of Lys and Tb-LDH. However, the reflectance spectra of Tb-LDH/Lys-*n*(*n* = 1,2,3,4,5) composites are different from those of Lys, Tb-LDH, and mixture of Tb-LDH/Lys. The band-edge of the Tb-LDH/Lys-1 is close to that of the Tb-LDH. With increasing Lys adsorbed in the Tb-LDH, the band-edge of Tb-LDH/Lys-n shifted to low energy, and the reflectance spectrum profile is more similar to that of the Lys. Moreover, the reflectance spectra of Tb-LDH/Lys-n are obviously different from that physical mixture of Tb-LDH/Lys, indicating interaction between Tb-LDH and Lys present in the Tb-LDH/Lys-*n*. The present fluorescent quenching may be due to the interaction. In view of the difficult coordination of Tb^{3+} and -NH_2 or -COOH group of lysine due to the blocking of OH groups in the layers, there may be no direct coordination between the lysine and Tb-LDH. Therefore, the fluorescent change is possibly relevant to other interaction, such as the hydrogen-bonding interaction or electrostatic interaction between NH_2 (or COOH) groups of Lys (lysine) and the OH groups on the layers of LDH. This interaction lead to energy transfer from the $^5D_4$ (Tb^{3+}) state to the lowest triplets of the lysine, accordingly lead to quenching of Tb^{3+} green emission.

Conclusions

The green emission of Tb-doped LDH response to lysine has been investigated. The green emissions due to the $^5D_4$–^7F_J (J = 3, 4, 5, 6) transitions of Tb-LDH markedly decreased after the Tb-doped LDH was exposed to lysine solution. Compositional analyses suggested that the content of lysine present in the Tb-LDH/Lys composites gradually increased with increasing concentration of lysine solution. The green emission of Tb-LDH optimal response to lysine happened at 0.05 mol·L^{-1} of lysine. This fluorescence of Tb-LDH sensitive to low concentration of lysine would be potential application in biological fluorescent prober.

Acknowledgments The Project was supported by the National Natural Science Foundation of China (Grant No.51162021).

References

1. Carpenter KJ, Booth VH (1973) Damage to lysine in food processing: its measurements and its significance. Nutr Abstr Rev 43:423–428
2. Moore S, Spackmann DH, Stein WH (1958) Automatic recording apparatus for use in the chromatography of amino acids. Anal Chem 30(7):1185–1189
3. Rutherfurd SM, Rutherfurd-Markwick KJ, Moughan PJ (2007) Available (ileal digestible reactive) lysine in selected pet foods. Agri Food Chem 55(9):3517–3522
4. Rutherfurd SM, Moughan PJ (1997) Application of a new method for determining digestible reactive lysine to variably heated protein sources. Agric Food Chem 45(5):1582–1586
5. Rutherfurd SM, Torbatinejad NM, Moughan PJ (2006) Available (ileal digestible reactive) lysine in selected cereal-based food products. J Agric Food Chem 54(25):9453–9457
6. Sun NQ, Li LP, Yang YM, Zhang AQ, Jia HS, Liu XG, Xu BS (2015) Synthesis, characteristics and luminescent properties of a

new Tb(III) ternary complex applied in near UV-based LED. Optl Mater 49:39–45
7. Choi Y, Yoon Y, Kang JG, Sohn Y (2015) Photoluminescence imaging of Eu(III) and Tb(III)-embedded SiO_2 nanostructures. J Lumin 158:27–31
8. Essawy AA, Afifi MA, Moustafa H, El-Medani SM (2014) DFT calculations, spectroscopic, thermal analysis and biological activity of Sm(III) and Tb(III) complexes with 2-aminobenzoic and 2-amino-5-chloro-benzoic acids. Spectrochim Acta A 131:388–397
9. Lee HS, Spraggon G, Schultz PG, Wang F (2009) Genetic incorporation of a metal-ion chelating amino acid into proteins as a biophysical probe. J Am Chem Soc 131(7):2481–2483
10. Zhao MM, Tang RR, Xu SA (2015) Investigations into the bovine serum albumin binding and fluorescence properties of Tb (III) complex of a novel 8-hydroxyquinoline ligand. Spectrochim Acta A 35: 953–958
11. Chen YF, Zhou SH, Li F, Chen YW (2010) Synthesis and photoluminescence of Eu-doped Zn/Al layered double hydroxides. J Mater Sci 45:6417–6423
12. Chen YF, Li F, Zhou SH, Wei JC, Dai YF, Chen YW (2010) Structure and photoluminescence of Mg–Al–Eu ternary hydrotalcite-like layered double hydroxides. J Solid State Chem 183:2222–2226
13. Chen YF, Li F, Zhou SH, Wei JC, Dai YF, Chen YW (2012) The fluorescence of Mg–Al–Eu ternary layered hydroxides response to tryptophan. Luminescence 27:223–228
14. Chen YF, Li F, Yu GS, Yang XJ (2012) Fluorescence of Zn-Al-Eu ternary layered hydroxides response to phenylalanine. Spectrochim Acta A 86:625–630
15. Bach LG, Islam MR, Cao XT, Park JM, Lim KT (2014) A novel photoluminescent nanohybrid of poly(e-caprolactone) grafted Mg/Al layered double hydroxides and Tb^{3+} ions: synthesis and characterization. J Alloys Compds 582:22–28
16. Zhuravleva NG, Eliseev AA, Lukashin AV, Kynast U, Tretyakov YD (2004) Energy transfer in luminescent Tb- and Eu-containing layered double hydroxides. Mendeleev Commun 14(4):176–178
17. Wang LJ, Xu XY, Evans DG, Duan X, Li DQ (2010) Synthesis and selective IR absorption properties of iminodiacetic-acid intercalated MgAl-layered double hydroxide. J Solid State Chem 183:1114–1119
18. Mo ZL, Gou H, He JX, Yang PP, Feng C, Guo RB (2012) Controllable synthesis of functional nanocomposites: covalently functionalize grapheme sheets with biocompatible L-lysine. Appl Surf Sci 258:8623–8628
19. Kang NJ, Wang DY, Kutlu B, Zhao PC, Leuteritz A, Wagenknecht U, Heinrich G (2013) A new approach to reducing the flammability of layered double hydroxide (LDH)-based polymer composites: preparation and characterization of dye structure-intercalated LDH and its effect on the flammability of polypropylene-grafted maleic anhydride/d-LDH composite. ACS Appl Mater Interfaces 5:8991–8997
20. Mészáros S, Halász J, Kónya Z, Sipos P, Pálinkó I (2013) Reconstruction of calcined MgAl- and NiMgAl-layered double hydroxides during glycerol dehydration and their recycling characteristics. ApplClay Sci 80(81):245–248
21. Lennerová D, Kovanda F, Brožek J (2015) Preparation of Mg–Al layered double hydroxide/polyamide 6 nanocomposites using Mg–Al–taurate LDH as nanofiller. Appl Clay Sci 114:265–272
22. Kumar P, Gill K, Kumar S, Ganguly SK, Jain SL (2015) Magnetic Fe_3O_4@MgAl–LDH composite grafted with cobaltphthalocyanine as an efficient heterogeneous catalyst for the oxidation of mercaptans. J Mole Catal A: Chem 401:48–54
23. Wang JG, Wei Y, Yu J (2013) In fluences of polyhydric alcohol co-solvents on the hydration and thermal stability of MgAl-LDH obtained via hydrothermal synthesis. Appl Clay Sci 72:37–43
24. Phuong NTK (2014) Entrapment of Mg − Al layered double hydroxide into alginate/polyvinyl alcohol beads for water remediation. J Envirol Chem Eng 2:1082–1087
25. Kameda T, Fubasami Y, Uchiyama N, Yoshioka T (2010) Elimination behavior of nitrogen oxides from a NO_3^--intercalated Mg–Al layered double hydroxide during thermal decomposition. Thermochim Acta 499:106–110
26. Li F, Zhang LH, Evans DG, Forano C, Duan X (2004) Structure and thermal evolution of Mg–Al layered double hydroxide containing interlayer organic glyphosate anions. Thermochim Acta 424:15–23
27. Petrosyan AM, Ghazaryan VV (2009) Vibrational spectra of L-lysine monohydrochloride dihydrate and its two anhydrous forms. J Mole Struct 917:56–62
28. Yoo EJ, Chae B, Jung YM, Lee SW (2015) pH-induced structural changes of surface immobilized poly(L-lysine) by two-dimensional (2D) infrared correlation study. Chin Chem Lett 26:173–176
29. Kitadai N, Yokoyama T, Nakashima S (2009) ATR-IR spectroscopic study of L-lysine adsorption on amorphous silica. J Colloid Interf Sci: 31–37.
30. Kitadai N, Yokoyama T, Nakashima S (2009) In situ ATR-IR investigation of L-lysine adsorption on montmorillonite. J Colloid Interf Sci 338:395–401
31. Aydın M, Kartal Z, Osmanoglu S, Halim Baskan M (2011) Ramazan Topkaya, EPR and FT-IR spectroscopic studies of L-lysine monohydrochloride and L-glutamic acid hydrochloride powders. J Mole Struct 994:150–154
32. Sas EB, Kose E, Kurt M, Karabacak M (2015) FT-IR, FT-Raman, NMR and UV–vis spectra and DFT calculations of 5-bromo-2-ethoxyphenylboronic acid (monomer and dimer structures). Spectrochim Acta A 137:1315–1333
33. Larin AV, Bryukhanov IA, Rybakov AA, Kovalev VL, Vercauteren DP (2013) Theoretical identification of carbonate geometry in zeolites from IR spectra. Micropor Mesopor Mater 173:15–21
34. Delgado RR, Pauli CPD, Carrasco CB, Avena MJ (2008) Influence of M^{II}/M^{III} ratio in surface-charging behavior of Zn–Al layered double hydroxides. Appl Clay Sci 40:27–37
35. Gutzov S, Bredo M (2006) Preparation and luminescence of terbium and cerium-doped silica xerogels. J Mater Sci 41:1835–1837
36. Sohn Y (2014) Structural and spectroscopic characteristics of terbium hydroxide/oxide nanorods and plates. Ceram Internat 40: 13803–13811
37. JyothyPV AKA, Gijo J, Unnikrishnan NV (2009) Fluorescence enhancement in Tb^{3+}/CdS nanoparticles doped silica xerogels. J Fluoresc 19:165–168
38. Davesnne C, Ziani A, Labbé C, Marie P, Frilay C, Portier X (2014) Thin Solid Films 553: 33–37.
39. Souza AS, Nunes LA, Felinto MCFC, Brito HF, Malta OL (2015) On the quenching of trivalent terbium luminescence by ligand low lying triplet state energy and the role o fthe $^7F_5$ level:the[$Tb(tta)_3(H_2O)_2$] case. J Lumin 167:167–171
40. Khan MN, Shah J, Jan MR, Lee SH (2013) AValidated spectrofluorimetric method for the determination of citalopram in bulk and pharmaceutical preparations based on the measurement of the silver nanoparticles-enhanced fluorescence of citalopram/terbium complexes. J Fluoresc 23:161–169
41. Onoda H, Funamoto T (2015) Preparation and fluorescence properties of crystalline gel rare earth phosphates. J Fluoresc 25:247–251
42. Youssef AO (2012) Spectrofluorimetric assessment of hydrochlorothiazide using optical sensor Nano-composite terbium ion doped in sol-gel matrix. J Fluoresc 22:827–834
43. Souza ER, Zulato CHF, Mazali IO, Sigoli FA (2013) Synthesis and photoluminescent properties of lanthanides acetoacetanilide complexes. J Fluoresc 23:939–946

44. Ye ZQ, Xiao YN, Song B, Yuan JL (2014) Design and synthesis of a new terbium complex-based luminescent probe for time-resolved luminescence sensing of zinc ions. J Fluoresc 24:1537–1544
45. Wankar S, Limaye SN (2015) Luminescence and electronic spectral studies of some synthesized lanthanide complexes using benzoic acid derivative and o-phenanthroline. J Fluoresc 25:787–794
46. Li WX, Li YJ, Chai WJ, Ren T, Liu Y, Zhang J, Ao BY (2012) Syntheses and fluorescence properties of two novel lanthanide (III) perchlorate complexes with Bis(benzylsulfinyl) methane. J Fluoresc 22:651–658
47. An XP, Wang HS, Li GC (2014) Structures and luminescent properties of two 2D coordination polymers containing Tb(III) or Dy(III) ions. J Fluoresc 24:425–429
48. Qian XM, Gong WT, Wang FR, Lin Y, Ning GL (2015) A pyrylium-based colorimetric and fluorimetric chemosensor for the selective detection of lysine in aqueous environment and real sample. Tetrahedron Lett 56:2764–2767
49. Cao JH, Ding LP, Zhang YY (2016) Shihuai Wang, Yu Fang, a ternary sensor system based on pyrene derivative-SDS assemblies-Cu 2+ displaying dual responsive signals for fast detection of arginine and lysine in aqueous solution. J Photochem Photobio A: Chem 314:66–74
50. Safiullin GM, Nikiforov VG, Davydov NA, Mustafina AR, Soloveva SY, Lobkov VS, Salikhov KM, Konovalov AI (2015) Detailed mechanism of the ligand-to-metal energy transfer of silica-coated Tb(III) complex with p-sulfonatothiacalix[4]arene. J Lumin 157:158–162
51. Sun NQ, Li LP, Yang YM, Zhang AQ, Jia HS, Liu XG, Xu BS (2015) Synthesis, characteris tics and luminescent properties of a new Tb(III) ternary complex applied in near UV-based LED. Opt Mater 49:39–45
52. Bünzli J-C G (2015) On the design of highly luminescent lanthanide complexes. Coord Chem Rev 293(294):19–47
53. Binnemans K (2009) Lanthanide-based luminescent hybrid materials. Chem Rev 109:4283–4374
54. Zhuravlev KP, Kudryashova VA, Tsaryuk VI (2016) Luminescence and energy transfer processes in europium and terbium complexes with 2-substituted cycloalkanones and 1,10-phenanthroline derivatives. J Photochem Photobio A: Chem 314:14–21
55. Wang Y, Jiang ZH, Lv YG, Zhang YJ, Ma DY, Zhang FJ, Tan B (2011) Study of synthesis and luminescent properties of a novel terbium rare earth complex $Tb(PCAD)_3$ Phen. Synth Met 161: 655–658